Bull Volcanol (2010) 72:449–467
DOI 10.1007/s00445-009-0330-6

RESEARCH ARTICLE

Explosive lava–water interactions I: architecture and emplacement chronology of volcanic rootless cone groups in the 1783–1784 Laki lava flow, Iceland

Christopher W. Hamilton · Thorvaldur Thordarson · Sarah A. Fagents

Received: 22 May 2009 / Accepted: 1 December 2009 / Published online: 3 February 2010

Abstract To determine the relationships between rootless cone emplacement mechanisms, morphology, and spatial distribution, we mapped the Hnúta and Hrossatungur groups of the 1783–1784 Laki lava flow in Iceland. We based our facies maps on Differential Global Positioning System (DGPS) measurements, photogeological interpretations, and supporting field observations. The study area covers 2.77 km^2 and includes 2216 explosion sites. To establish the timing of rootless cone formation we incorporated tephrochronological constraints from eighty-eight stratigraphic sections and determined that the Hnúta and Hrossatungur groups are composite structures formed by the emplacement of six geographically and chronologically discrete domains. Rootless eruptions initiated in domain 1 on the first day of the Laki eruption (June 8, 1783) and lasted 1–2 days. The second episode of rootless activity began in domain 2 on June 11 and lasted 1–3 days. The four domains of the Hrossatungur group dominantly formed after June 14 and exhibit a complex emplacement sequence that reflects interactions between the Laki lava, contemporaneously emplaced rootless cones, and an existing topographic ridge. In the study area, we identify three distinct rootless cone archetypes (i.e., recurring morphological forms) that are related to tube-, channel-, and broad sheet lobe-fed eruptions. We assert that emplacement of lava above compressible substrates (e.g., unconsolidated sediments) may trigger rootless eruptions by causing subsidence-induced flexure and failure of the basal crust, thereby allowing molten lava (fuel) to come into direct contact with groundwater (coolant) and initiating analogs to explosive molten fuel–coolant interactions (MFCIs).

Keywords Volcanic rootless cones · Pseudocraters · Phreatomagmatic · Explosive lava–water interactions · Laki · Iceland · Mars

Editorial responsibility J. White

Electronic supplementary material The online version of this article (doi:10.1007/s00445-009-0330-6) contains supplementary material, which is available to authorized users.

C. W. Hamilton (✉) · S. A. Fagents
Hawai'i Institute of Geophysics and Planetology,
University of Hawai'i,
1680 East-West Road,
Honolulu, HI 96822, USA
e-mail: christopher@higp.hawaii.edu

T. Thordarson
School of Geosciences, University of Edinburgh,
Edinburgh, Scotland, UK

Introduction

Volcanic rootless cones, also known as pseudocraters, result from explosive interactions between lava and water-bearing substrates (Thorarinsson 1951, 1953). On Earth, explosive lava–water interactions generally occur within littoral environments, lacustrine basins, riverbeds, mires, and glacial outwash plains (Fisher 1968; Mattox and Mangan 1997; Fagents and Thordarson 2007). Terrestrial rootless cone groups cover areas of approximately 0.5–150 km^2 and are composed of numerous conical landforms ranging 1–35 m in height and 2–450 m in basal diameter (Fagents and Thordarson 2007).

The study of explosive lava–water interactions has broad implications for understanding phreatomagmatic eruption processes, volcanic hazards, paleo-environments, and planetary surface processes. Rootless eruptions provide excellent natural analogs to experimental molten fuel–coolant interactions (MFCIs; e.g., Colgate and Sigurgeirsson 1973; Wohletz 1983, 1986, 2002; Wohletz and Sheridan 1983; Zimanowski et al. 1991; Zimanowski 1998; Morrissey et al. 2000) because the lava (i.e., fuel) has undergone an initial stage of degassing

at the vent and, therefore, pyroclastic fragmentation and tephra dispersal are purely driven by thermal expansion of external water (i.e., coolant). Rootless MFCIs can pose significant hazards because of their sudden initiation and capacity for widespread tephra dispersal (Thordarson et al. 1998a). Rootless cones are paleo-environmental indicators because their occurrence implies the presence of water within the near-surface substrate at the time of the explosive lava–water interactions. Consequently, analogs to Icelandic rootless cones at mid-latitudes on Mars (Allen 1979; Frey et al. 1979; Frey and Jarosewich 1982; Lanagan et al. 2001; Greeley and Fagents 2001; Fagents et al. 2002; Fagents and Thordarson 2007) support the hypothesis that near-equatorial groundwater (or ice) has been present in the Martian regolith during the geologically recent past (i.e., <10 Myr), despite the fact that under current climate conditions ground ice is not expected to be stable at latitudes less than 40–50° (Squyres et al. 1992; Mellon and Jakosky 1995).

The purpose of this study is to constrain the emplacement conditions, timing, and spatial distribution of the rootless cones in the Hnúta and Hrossatungur groups of the 1783–1784 Laki lava flow in Iceland. This information provides new insights into the architecture of rootless cone groups and their emplacement chronology. These results are important for assessing hazards associated with explosive lava–water interactions because they establish constraints on the duration of rootless eruptions and their delayed onset after initial lava emplacement. The rootless cone archetypes defined within this study also have broader implications because they are useful for identifying the products of explosive lava–water interactions in other locations and for interpreting the paleo-environmental significance of rootless cone groups in volcanic regions on Earth and Mars. Field-based identification of rootless eruption sites and the internal boundaries within rootless cone groups, allows us to apply sample-size-dependent nearest neighbor analyses to investigate how competitive resource utilization can lead to self-organization within geological systems (Hamilton et al. 2010). This study is therefore relevant to understanding MFCI triggering mechanisms in natural environments, mitigating volcanic hazards, investigating paleo-environments, examining planetary surfaces processes, establishing non-morphological criteria for identifying landforms in remote sensing data, and modeling self-organization processes within geological systems.

Background information

Review of previous research

Rootless eruptions commonly occur in littoral environments where lava advances over water-saturated sediments—as demonstrated by eyewitness accounts of the 1868 Pu‘u Hou event on the southwest coast of Mauna Loa, Hawai‘i (Brigham 1868). Along coastlines, littoral explosions typically generate radial distributions of tephra with approximately half of the material falling into the sea and the other half constructing crescent-shaped ridges on stable landward surfaces (Fisher 1968; Fisher and Schmincke 1984). Radially symmetric cones can also form in near-coastal environments where tephra is deposited onto stable lava surfaces due to explosive interactions between water-saturated hyaloclastite deltas and overlying lava tubes (Jurado-Chichay et al. 1996). If littoral explosions occur in association with lava channels, then tephra may be deposited onto the moving lava surface and rafted to sea, thereby forming paired half-cone deposits on either side of active channels, or paired quarter-cone deposits if the seaward halves of the cones are not preserved (Fisher 1968; Mattox and Mangan 1997).

Rootless eruptions have been observed in Iceland during the 1783–1784 Laki eruption when lava inundated lacustrine basins near the mouth of the Skaftá River gorge (Steingrímsson and Ólafsson 1783; Steingrímsson 1788). The secondary origin of other cone groups in Iceland was recognized by Pálsson (1794) and Robert (1840), but neither identified the mechanisms by which they formed. Thoroddsen (1879, 1894)—inspired by news of littoral eruptions in Hawai‘i—first proposed that rootless cone groups in Iceland formed by explosive interactions between hot lava and near-surface water. Thorarinsson (1951, 1953) confirmed this hypothesis by documenting a secondary tephra layer, traceable for more than 0.5 km, around a rootless cone group in the ~2.3 ka Younger-Laxárdalur lava flows in northern Iceland. Furthermore, he showed that the flowing lava did not deform any of the rootless cones, nor was the lava path deflected by the cones. These observations, among others, led Thorarinsson to conclude that the rootless cones were emplaced concurrently with their host lava flows, and the volatile phase driving the explosive activity was water vapor trapped beneath the flows.

The hypothesis proposed by Thorarinsson (1951, 1953) appears to offer an explanation for the origin of rootless cone groups. However, his theory implies rootless eruptions are triggered by phreatic explosions that initiate due to conductive heat transfer from hot lava to an underlying water reservoir that is trapped below the active flow. Thermal conduction and water vaporization must therefore continue until the vapor pressure exceeds the mechanical strength of the lava flow and its overburden pressure. The conductive heat transfer model fails to explain: (1) how efficient heat transfer can be maintained through a thickening vapor film that would insulate the base of the lava from the underlying liquid water due to the Leidenfrost effect; (2) field observations that provide evidence for intimate mingling of fluidal lava and substrate sediments within the opening phases of rootless eruptions; and (3) the

physical conditions required to sustain rootless eruptions to produce well-bedded tephra successions. To address these issues, Fagents and Thordarson (2007) asserted that dynamic heat transfer mechanisms are required to physically mix lava and water-saturated sediments and thus initiate analogs to explosive MFCIs. Rootless eruptions therefore involve cyclic pulses of explosive activity that are fed by lateral flow of lava to the eruption site through prefered pathways (e.g., lava tubes or channels) until either the lava supply dwindles, or the underlying groundwater resources are exhausted.

The Laki eruption and geological context of the study area

The Laki eruption occurred in southern Iceland (Fig. 1) during an eight month period beginning at 9:00 A.M. on June 8, 1783 and continuing until February 7, 1784. The eruption produced 15.1±1 km^3 of dense rock equivalent (DRE) tholeiitic magma, of which 14.7 km^3 was emplaced as lava and 0.4 km^3 as tephra (Thordarson and Self 1993; Thordarson et al. 1996). The eruption occurred along ten *en echelon* fissure segments that sequentially opened toward the northeast to produce a 27 km-long cone row. The fissure system comprises >140 primary eruption sites—including scoria cones, spatter cones, and tuff cones (Fig. 1). The ten fissure segments opened during the first five months of the eruption and each was associated with a short-lived (0.5–4 day) subplinian phase, followed by a longer lava effusion phase. The eruption produced 10–13 km-high eruption columns that infused volcanic ash and ~100 Mt of SO_2 into the polar jet stream to produce a net eastward dispersion of the plumes (Thordarson et al. 1996). These sulfur emissions produced ~200 Mt of H_2SO_4 aerosols, which maintained a sulfuric aerosol veil over the Northern Hemisphere and caused climate perturbations for 2–3 years (Thordarson and Self 2003).

The Laki lava flow field covers 599 km^2 and consists of two major domains: Eldhraun to the west, and Brunahraun

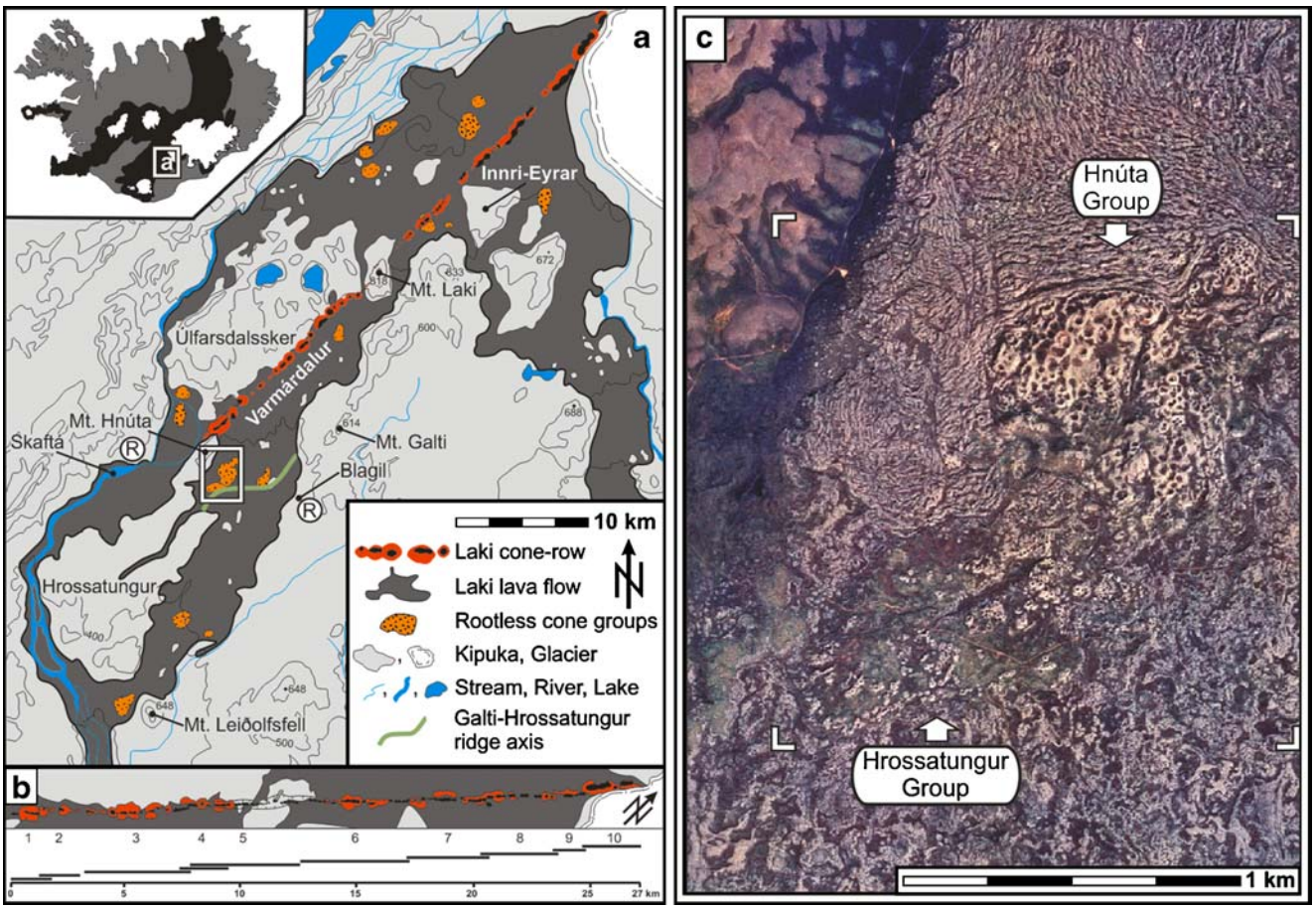

Fig. 1 Study area location within the active volcanic zones (black) of Iceland (*Inset*). **a** Geological map of the Laki cone row and surrounding lava flow field. The box shows the main study area (**c**), which is located at the southern end of Varmárdalur—near the crest of the Galti-Hrossatungur ridge (green). "R" denotes the location of regional tephra reference sections used within this study. **b** Fissure segments of the Laki vent system are labeled 1–10 in accordance with their sequence of formation. **c** Orthogonal color aerial photograph (0.5 m/pixel) showing the Hnúta and Hrossatungur groups. The four white corners denote the extent of Fig. 3

to the east. Eldhraun features two main branches, one confined to the Skaftá River gorge and another extending across the Síða highlands, from Mt. Galti to Mt. Leiðólfsfell (Fig. 1a). Lava entering the Skaftá River gorge primarily originated from fissure segments 1 and 2, whereas the Síða branch was fed by lava flowing southwards from fissure segments 1–5 (Fig. 1b). The presence of >16 rootless cone groups within the Laki lava flow field (Fig. 1a) implies a high water table in the region. This interpretation is consistent with contemporary descriptions (Steingrímsson and Ólafsson 1783), which state that in the vicinity of Laki there were extensive wetlands and swan nesting grounds in the Varmá Valley (i.e., Varmárdalur in Icelandic). Prior to the Laki eruption, the southern margin of Varmárdalur was blocked by a 40–50 m-high antiform, hereafter termed the Galti-Hrossatungur ridge (Fig. 1a).

Nomenclature

To facilitate further discussion of rootless tephra deposits, we define the following nomenclature. Rootless tephra is the generic term for all pyroclasts formed by explosive lava–water interactions. Rootless explosions initiate in a zone beneath the lava flow termed a rootless eruption site. A rootless eruption site extends from the substrate, through the lava flow, and to the surface via a rootless conduit and vent. Rootless vents have a funnel shape that widens towards the surface, but in cross-section they may exhibit irregular margins within the host lava flow—as evidenced in river-cut exposures through the Thjórsárdalur rootless cone group in Iceland. The perimeter of a rootless vent is expressed at the surface as the rim of a crater. Crater rims are commonly circular in plan view; however, superimposed craters may generate non-circular geometries. A rootless crater floor is the lowermost surface exposed within a rootless eruption crater. Rootless craters may have one or more crater floors depending on the number of underlying eruption sites and the vent infilling history.

Rootless tephra deposits typically include three facies (Fig. 2a): (1) a distal fall deposit with a sheet-like geometry that results from widespread tephra deposition from a weak convective plume; (2) a tephra platform formed by

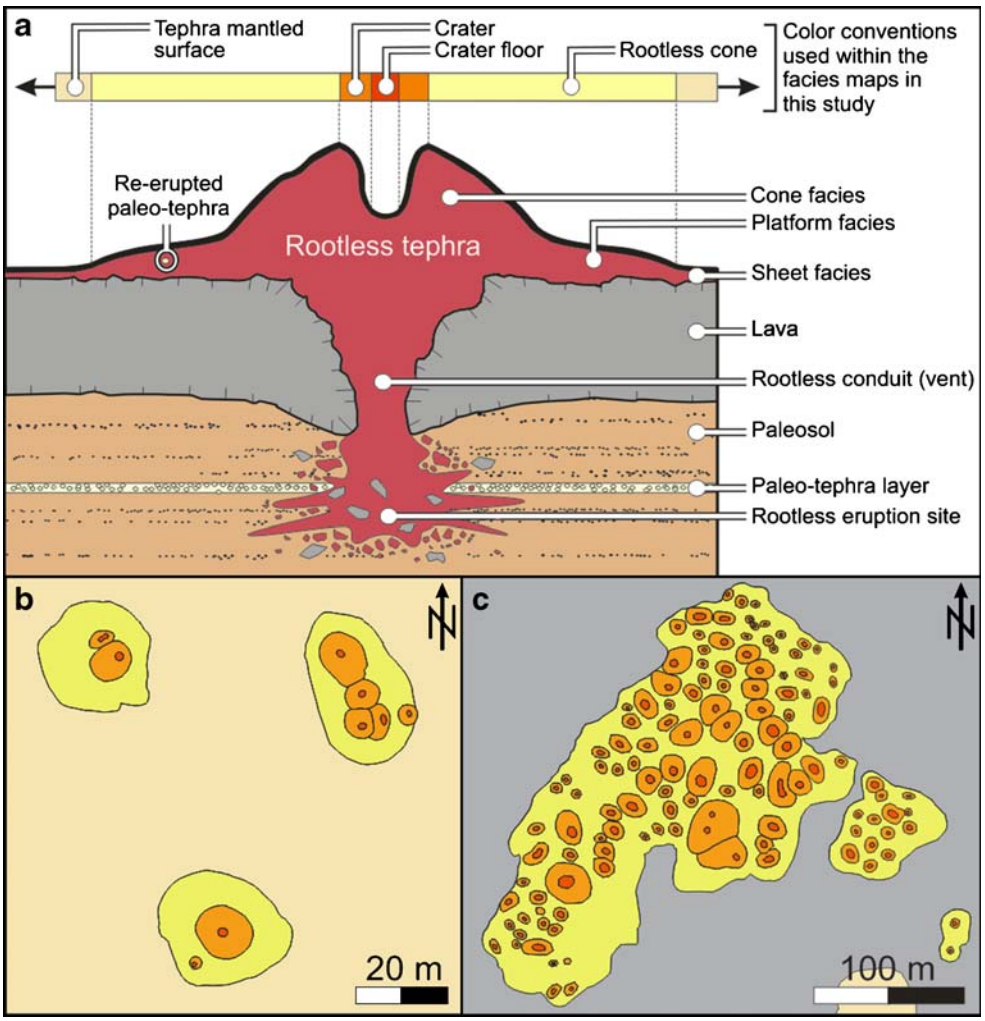

Fig. 2 Conceptual model of rootless cone facies. **a** Rootless tephra deposits typically include three morphological subdivisions: distal sheet-like fall deposits, an intermediate tephra platform, and a proximal cone-shaped accumulation of tephra with a central crater above a rootless vent. Tephra deposits formed in association with one dominant rootless explosion site tend to exhibit radial symmetry (**b**); however, as the number of rootless eruption sites increases so does the morphological complexity of the rootless tephra deposit (**c**). **b** and **c** are plan view facies maps extracted from the study area

intermediate fall deposits, and in some instances, surge deposits; and (3) vent-proximal tephra deposits that accumulate to form a steeply dipping cone surrounding a central crater. In general, rootless tephra has a modal grain-size of ash in the distal sheet-like deposits, ash to lapilli in the tephra platforms, and lapilli to bombs in the vent-proximal cones. Rootless tephra is typically unconsolidated except within the proximal deposits, which commonly include reversely-graded bedding sequences with spatter-rich layers that may exhibit welding and, in some instances, rheomorphic flow. Rootless tephra deposits tend to contain a significant fraction of substrate material ranging from clay to cobbles, depending on the nature of the underlying sediments.

If rootless tephra is dispersed from a single eruption site and deposited onto a stationary surface, the resulting landform will typically exhibit radial symmetry (Fig. 2b). Rootless tephra deposits may form more complex morphologies due to overlapping and interfingered deposits from multiple eruption sites (Fig. 2c). We term the latter features rootless tephra complexes. In some cases (e.g., the Hnúta group), rootless tephra complexes may develop a single platform with ill-defined margins between clearly expressed craters.

The term rootless cone group broadly refers to an assemblage of rootless tephra deposits that concentrate within a geographic region (e.g., Fig. 1a depicts 16 rootless cone groups near the Laki cone row). A major conclusion of this study is that rootless cone groups are composite structures constructed during discrete episodes of rootless eruption activity. We subdivide contemporaneously emplaced rootless cones group into domains. For instance, we identify six domains in the Hnúta and Hrossatungur groups based on their spatial distribution, superpositioning relationships, and tephrostratigraphy ("Emplacement chronology of rootless cones within the Hnúta and Hrossatungur groups"). To explore local emplacement processes, we also define subdomains, which include >30 rootless eruption sites—all of which exhibit a close spatial association and strong evidence for contemporaneous formation. The groups, domains, and subdomains introduced in this study are utilized by Hamilton et al. (2010) to quantify the spatial distribution of rootless eruption sites and investigate processes of self-organization at different scales.

Methods

This study develops two lines of enquiry: (1) facies mapping using Differential Global Positioning System (DGPS) measurements, remote sensing, and Geographic Information Systems (GIS); and (2) field observations of rootless tephra deposits, morphologies and contact relationships. We conducted field work within the Hnúta and Hrossatungur groups during the summers of 2004–2008. During this time, DGPS measurements of latitude, longitude, and elevation were used to delimit all geological units (e.g., lava flow margins, kipuka, etc.) and morphological transitions (e.g., slope breaks marking the base of each rootless cone, crater rim, and crater floor) within the study area. DGPS records were typically obtained along duplicated traverses using two Ashtech Z-Xtreme receivers—one operating as a static base-station and the other as a kinematic rover. Appendix 1 summarizes the DGPS post-processing methodology and evaluation of data precision. The resulting dataset includes 1,319,844 kinematic DGPS measurements with an absolute deviation (i.e., precision) ranging from ±0.06 m to ±0.08 m for duplicated and single traverses, respectively.

In ArcGIS, DGPS tracks and handheld GPS observation sites were superimposed on digital color aerial photographs with a resolution of 0.5 m/pixel, and digitized to form a facies map covering an area of 2.77 km^2 (Fig. 3). The digital map and accompanying geospatial database contains 5,004 objects with eight feature classes (i.e., facies): (1) rootless cones; (2) craters; (3) crater floors; (4) incised cone margins; (5) tephra mantled surfaces; (6) kipuka; (7) lava; and (8) roads.

Field observations include documentation of the structure, morphology, and spatial distribution of rootless cones, lava flows, and kipuka. We established the emplacement chronology of the rootless cone domains using local superposition relationships coupled with tephrostratigraphy, which has been dated to the day for the Laki eruption using historical descriptions (Thordarson and Self 1993; Thordarson 2003; Thordarson et al. 2003). To identify pre-Laki eruption topography and develop stratigraphic correlations, we manually excavated eighty-eight pits ranging 0.25–2.18 m in depth. At each of these localities we identified tephra layers and compared them to the established tephrostratigraphy for the Laki eruption (Thordarson and Self 1993) and to two regional reference sections ("R" in Fig. 1a), which include historic tephra deposits ranging from the 870 Veiðivötn eruption to the 1918 eruption of Katla.

Results

Facies map

Rootless tephra deposits in the study area divide into six domains (Fig. 3). Domain 1 includes the main platform-shaped component of the Hnúta group and a series of satellite subdomains to the northwest. Domain 2 also belongs to the Hnúta group and it mantles the southern margin of domain 1 and an adjacent region to the south,

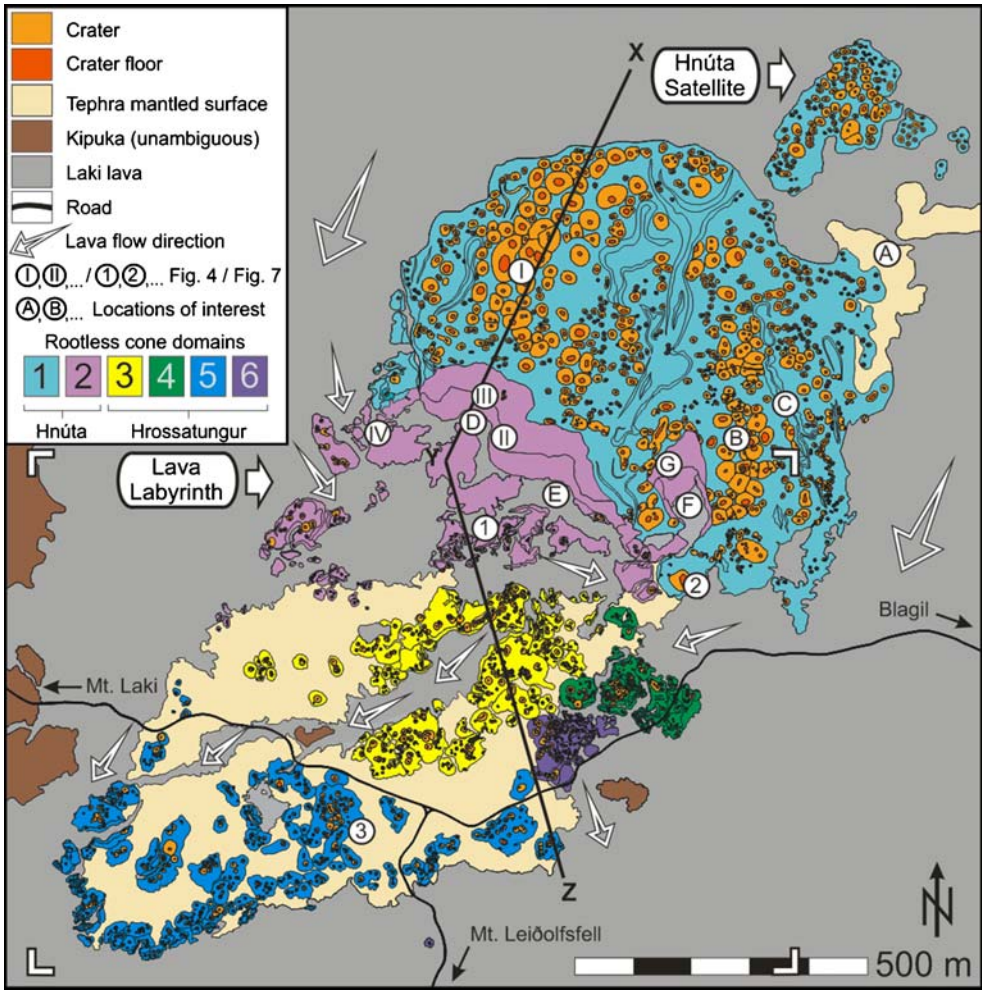

Fig. 3 Facies map depicting the six rootless cone domains within the Hnúta and Hrossatungur groups. **Domain 1** includes the platform of the main Hnúta group, and satellite subdomains extending northeast. **Domain 2** includes an arcuate ridge along the southern margin of the Hnúta group and an adjacent region, which we term the lava labyrinth. The Hrossatungur group consists of domains 3–6. **Domain 3** (containing subdomain 3.1) and **domain 5** (containing subdomain 5.1) are respectively located on the northern and southern slopes of the Galti-Hrossatungur ridge, whereas **domain 4** (containing subdomain 4.1) and **domain 6** (containing subdomain 6.1) are located along the eastern margin of the ridge. Mantled terrains are generally interpreted as kipuka; however, mantled terrains also include lava pathways that have been obscured by a veneer of tephra and reworked surface material. The four white corners delimit the extent of Fig. 5. Arrows indicate the approximate flow direction of the Laki lava. Roman numerals correspond to the location of field photographs (Fig. 4), tephra sections ("1", "2", and "3") are shown in Fig. 7. Profiles XY and YZ are illustrated in Fig. 8. Letters identify features of interest: tephra mantled surface ("A"), large rootless craters ("B"), channels formed by coalesced craters ("C"), rootless eruption sites ("D", "E", and "F"), and welded spatter deposits ("G"). See text for further details

which we term the lava labyrinth. Domains 3–6 combine to form the Hrossatungur group and they are all located to the south of the lava labyrinth. The overall study area includes 278 rootless cones, covering a total area of 619,423 m^2. The planimetric area of individual rootless cones within the Hnúta and Hrossatungur groups ranges from 1.61 m^2 to 390,224 m^2 with a mean of 2,228 m^2 (σ = ±329 m^2, σ_e = ±18 m^2). Within this study, population distributions tend to be highly asymmetric and thus, to prevent confusion when interpreting the significance of the mean, we report variations with both standard deviation, σ, and standard error of the mean, σ_e. This approach is advantageous because σ describes the variability between individuals in a sample whereas σ_e estimates how representative the sample mean is of the mean of the population from which the sample was drawn (n.b., σ_e equals σ divided by the square root of the number of samples in the distribution). There are a total of 2,038 rootless eruption craters and, assuming the properties of an equal area circle, these range 0.8–60.3 m in diameter with a mean of 8.1 m (σ = ±6.5 m, σ_e = ±0.2 m). The total number of crater floors (2,216) exceeds the number of craters because some of the rootless craters contain more than one explosion site.

Domain 1 The Hnúta group includes the oldest rootless cones in the study area—evidenced by the superposition relationships described below—and it divides into two principal regions: (1) a main cone complex (390,224 m^2) with an overall platform morphology; and (2) a group of satellite rootless tephra complexes (504 m^2 to 31,649 m^2).

Along the eastern margin of the Hnúta group there are several tephra-mantled surfaces with a southwest–northeast orientation ("A" in Fig. 3). The tephra mantles are too thick to allow us to determine the nature of the substrate, but the presence of cream colored pumice, not found within the primary Laki tephra deposits, suggests that the tephra mantle includes substrate material that was erupted from rootless sources within the adjacent Hnúta group and deposited onto a pre-eruption surface (i.e., the Galti-Hrossatungur ridge).

Domain 1 includes 680 craters ranging in diameter from 2.1–60.3 m (see "I" in Figs. 3 and 4), with a mean of 12.8 m (σ = ±8.3 m, σ_e = ±0.5 m). Deposits associated with the larger craters (e.g., "B" in Fig. 3) consist of ash to lapilli with blocky clasts, abundant clay- to sand-size sedimentary material, and foreign tephra (e.g., well-rounded, cream colored pumice grains that are 0.5–2.0 mm in diameter). Throughout the group, rootless craters exhibit north-south

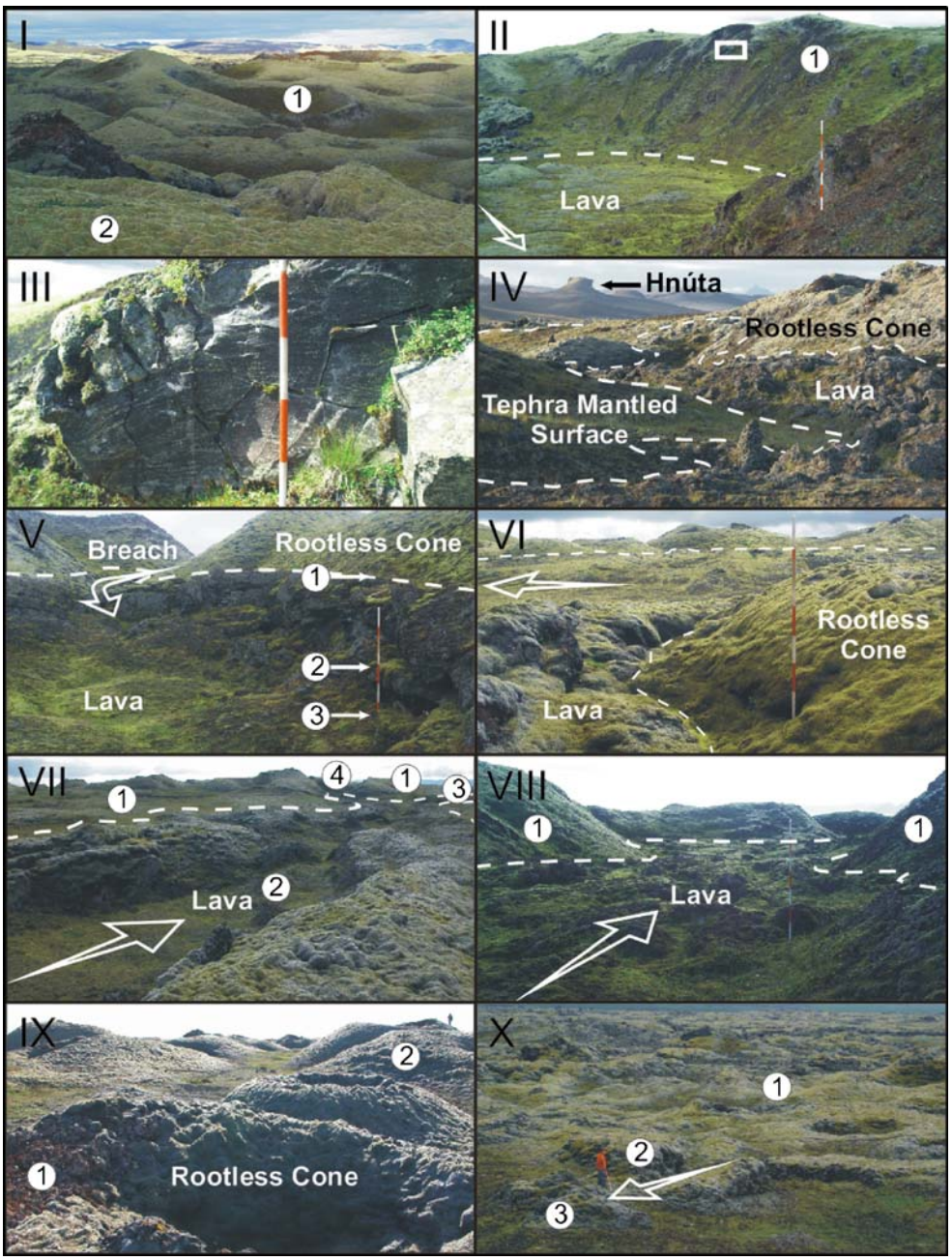

Fig. 4 **I:** "1" shows the surface of domain 1, whereas "2" shows part of the westernmost arcuate segment of domain 2. **II:** Westernmost arcuate segment ("1") with inset showing the location of III. **III:** Rheomorphic spatter horizon. **IV:** Lava labyrinth in the foreground with Mt. Hnúta in the background. **V:** A breach through the northern margin of domain 3. "1" corresponds to the lava high-stand whereas "2" and "3" show lava crusts formed after two lava drainage episodes. Large arrows show approximate lava flow directions. **VI:** Lava flow occupying the interior of domain 3. **VII:** Kipuka ("1"), confining a lava channel ("2") that divides into two branches: one flowing southwest ("3") and the other south ("4"). **VIII:** Elongate rootless cone with an axial trough ("1") that separates tephra that was emplaced on either side of a lava channel. **IX:** Ochre-colored rootless tephra ("1") coated in substrate sediments (i.e., clay). Tube-fed rootless cones ("2") exhibiting radial symmetry due to deposition of tephra onto a stationary lava crust. **X:** Small rootless cones in domain 6 ("1") with an example of a paired half-cone deposit produced by tephra deposition onto stationery channel levees ("2") and down-flow rafting of tephra ("3") that was deposited onto the surface of the active channel. The pole shown for scale is marked in 20 cm increments

alignments. Within domain 1, smaller rootless cones generally consist of lapilli- to bomb-sized spatter that partially covers tephra from the larger craters, thus indicating that the spattery cones are younger. The spatter-rich deposits are typically aligned along channels to form two parallel levees of rootless cone tephra with an axial depression between them that is V-shaped in cross-section (e.g., "C" in Fig. 3). Lava-rafted tephra commonly forms blockages within the channels in the down-flow direction. The Hnúta group ("I" in Figs. 3 and 4) forms a tephra platform that rises ~14 m above the surrounding lava flows.

Domain 2 Along the southern margin of the Hnúta group, the thickness of the tephra platform increases by ~16 m and, farther to the south, decreases by ~25 m ("II" in Figs. 3 and 4). These thickness variations occur over a distance of ~100 m, which imparts a ridge-like morphology to the southern part of the Hnúta group. The ridge consists of three arcuate segments that are concave towards the south and, from west to east, they are 188 m, 133 m, and 101 m wide (see the rootless cone deposits just north of the rootless eruption sites labeled "D", "E", and "F", respectively, in Fig. 3). The arcuate segments are composed of layered rootless tephra, which dominantly consists of unconsolidated juvenile ash to lapilli mixed with abundant sedimentary and foreign material. On the southern face of the ridge ("II" in Figs. 3 and 4), the succession features horizons of welded spatter and rheomorphic flows ("III" in Figs. 3 and 4). Well-bedded spatter deposits also cap the easternmost segment of the ridge ("G" in Fig. 3). Along the northern margin of domain 2, tephra belonging to the arcuate deposits infills adjacent explosion craters within domain 1, thus indicating that domain 2 is younger than domain 1.

The Hnúta group, including domains 1 and 2, deflected later lava flows to the southeast and southwest. The southwest branch was funneled between the Hnúta group and Mt. Hnúta and produced a labyrinthine network of rubbly pahoehoe flows with numerous kipuka and lava-inundated rootless cone remnants ("IV" in Figs. 3 and 4). The rootless tephra remnants include lava-rafted deposits and partially exposed cones associated with domain 2.

Domains 3–6 The Hrossatungur group extends south from the lava labyrinth and includes domains 3–6. There are 250 rootless cones and complexes within the Hrossatungur group. The total area of the group, excluding the tephra mantled surfaces between rootless cones, is 153,645 m^2. The area of individual rootless cones ranges 0.2–9,824 m^2 with a mean of 615 m^2 ($\sigma = \pm 99$ m^2, $\sigma_e = \pm 6.3$ m^2) Rootless cones within the Hrossatungur group include a total of 1,139 craters and 1,199 explosion sites. The crater diameters range 0.8–23.6 m in diameter with a mean of 5.2 m ($\sigma = \pm 2.7$ m, $\sigma_e = \pm 0.2$ m). Rootless cones in the Hrossatungur group show a statistically significant clustering relative to a Poisson random distribution (Hamilton et al. 2010) and can be divided into four distinct domains. Each of these domains include contemporaneously emplaced rootless cones that are separated from the other domains by kipuka containing continuous soil profiles that predate the Laki eruption.

In contrast to the Hnúta group, which exhibits an overall platform morphology, the Hrossatungur group includes three archetypical rootless cone morphologies: (1) radially symmetric rootless cones and elongate chains of cones; (2) paired half-cone deposits constructed on either side of lava channels; and (3) rootless tephra complexes. The study area also includes tumuli with rootless cone spatter deposits near their axial clefts (e.g., "H" in Fig. 5). Such tumuli are rare and do not constitute an independent archetype, but they do suggest that rootless cones can be genetically related to inflation features.

Domain 3 The oldest, and largest, rootless cone domain within the Hrossatungur group is located between the lava labyrinth and the Galti-Hrossatungur ridge ("I" in Fig. 5). In plan view, this domain has a U-shaped geometry that opens to the southwest. Subdomain 3.1 refers to the rootless cone complex in the southeastern region of the domain 3 ("S3.1" in Fig. 5). Subdomain 3.1 contains 65 explosion sites within 59 craters ranging 1.9–16.0 m in diameter with a mean of 6.7±3.0 m ($\sigma = \pm 3.0$ m, $\sigma_e = \pm 0.9$ m).

Rootless cone tephra generally covers the underlying lava flow except where the lava is exposed in a partially drained pond along the western margin of domain 3 ("J" in Fig. 5). The formation of domain 1 blocked the southern advance of the Laki lava and allowed the flow to accumulate to the north, within the lava labyrinth. The dammed flow continued to thicken and inundate local topographic lows along the northern slope of the Galti-Hrossatungur ridge (e.g., "K" in Fig. 5) until it overtopped the northeastern margin of domain 3 ("V" in Figs. 4 and 5). The lava from the breach overlies, and thus post-dates, the rootless cones within domain 3 ("VI" in Figs. 4 and 5). Lava was funneled from the breach into a topographic low defined by kipuka and the U-shaped interior of domain 3. The southward flow direction required that the lava move up-slope, towards the crest of the Galti-Hrossatungur ridge. The southward flow direction is evidenced by the southward dipping slope of the residual lava highstand along the margins of domain 3 and adjacent kipuka, counter-clockwise spinning lava-swirls along the left-bank of the lava channel ("L" in Fig. 5), and south to southwest dipping stalactites on the underside of drained lava crusts. These observations imply that as the flow thickened from the north, the lava advanced up-slope by progressively inundating new topographic lows at higher elevations. This

topographic low is now defined by kipuka on either side of the lava channel ("VII.1" in Fig. 4). The lava channel itself widens and deepens to the north (e.g., "L" in Fig. 5). Once the lava crossed the crest of the ridge ("M" in Fig. 5), the flow entered two topographic depressions ("VII.2" and "VII.3" in Fig. 4) that widen and deepen to the south. Lava crusts at two distinct levels below the highstand ("V" in Figs. 4 and 5) show that the channel drained in two discrete episodes, which presumably correspond to when the lava flooded into the two southward dipping topographic lows on the southern slope of the Galti-Hrossatungur ridge.

Domain 4 In contrast to domains 3 and 5, which were fed by lava that was deflected to the southwest by the Hnúta group, domain 4 is situated within the southeastern lava branch. The southeastern lava branch abuts a southeast-northwest trending landform that became a kipuka once it was surrounded by the Laki lava flow. The kipuka includes continuous soil sequences that pre-date the Laki eruption, outcrops of well-bedded palgonitized hyaloclastite (i.e., Möberg formations), and sedimentary deposits with low-angle aeolian cross-bedding and meltwater reworked material. These observations show that domains 3 and 4 formed within different lava lobes, are separated by kipuka, and thus had independent emplacement histories during the Laki eruption. Superposition relationships between domains 3 and 4 are ambiguous and it is not possible to distinguish their relative ages, but we conclude that they are of similar age because both are younger than domains 1 and 2, but older than domains 5 and 6. Subdomain 4.1 ("S4.1" in Fig. 5) contains 65 explosion sites within 54 craters ranging 1.5–14.2 m in diameter with a mean of

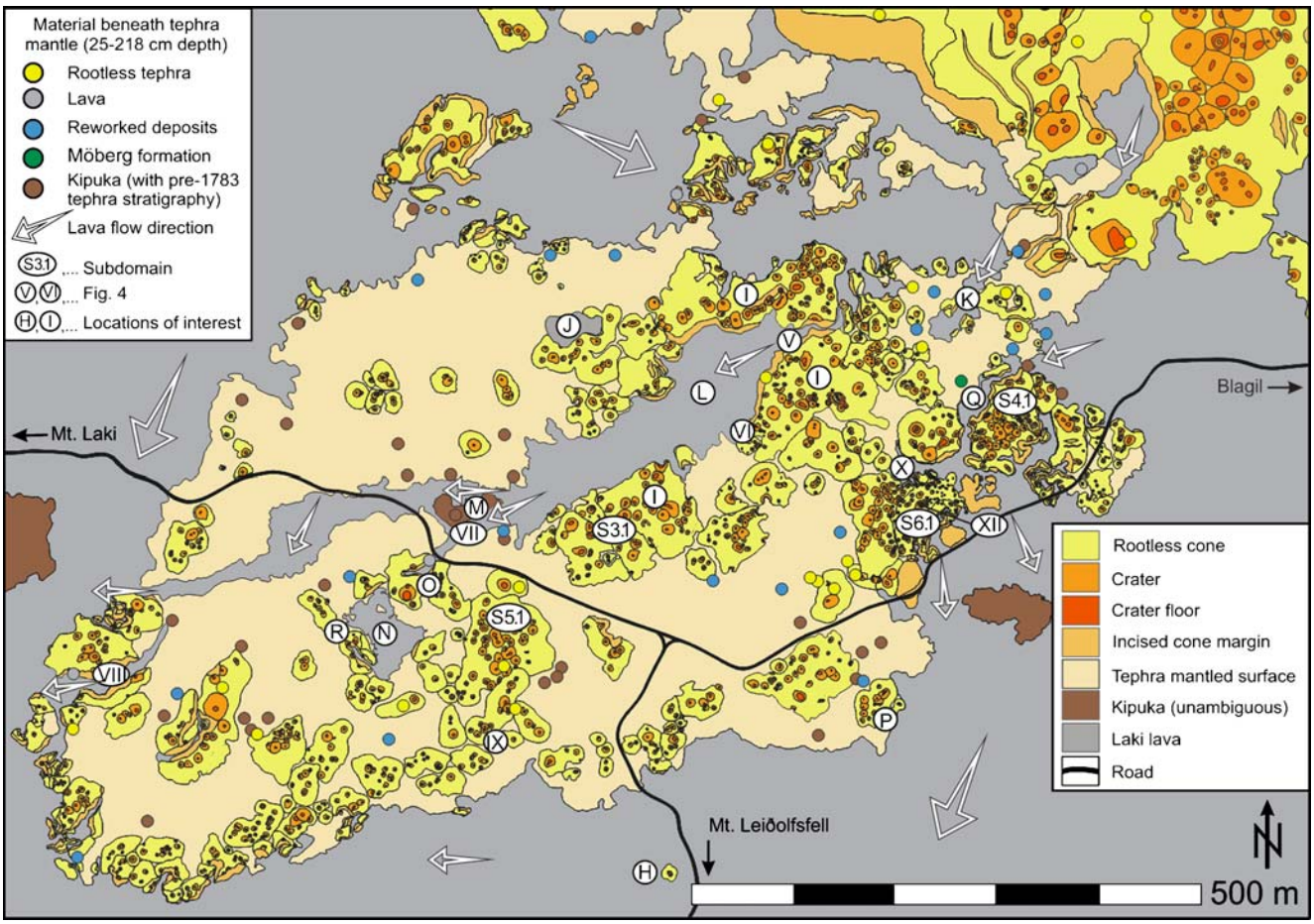

Fig. 5 Enlarged facies map of the Hrossatungur group showing the locations of 81 measured tephra sections. Yellow circles indicate primary rootless tephra, brown circles represent profiles into kipuka, green circles represent Möberg formations composed of well-bedded palagonitized hyaloclastite, blue circles show reworked material, and grey circles represent lava. Arrows indicate the approximate flow direction of the Laki lava. Roman numerals identify the location of field photographs (Fig. 4). Letters identify features of interest: tumulus with spatter deposits along its axial cleft ("H"); U-shaped rootless cone complex ("I"); ponded lava ("J"); lava-inundated gulley ("K"); lava channel ("L"); kipuka near the crest of the Galti-Hrossatungur ridge ("M"); pooled lava ("N"); paired half-cone deposit ("O"); peripheral rootless cone ("P"), lava channel abutting kipuka ("Q"); and transitional rootless cone archetype ("R"). "S3.1", "S4.1", "S5.1", and "S6.1" refer to subdomains within the four domains of the Hrossatungur group (see text for further details)

5.8 m (σ = ±2.3 m, σ_e = ±0.8 m). A chain of rootless eruption craters along the northern and western margins of subdomain 4.1 shows evidence of inundation by a later lava flow, which followed a counter-clockwise path towards the south. Upon emerging from the inundated section of domain 4, the lava flow generated a series of rootless eruptions to form domain 6.

Domain 5 After the flow emerged from domain 3 and crossed the crest of the Galti-Hrossatungur ridge, the lava divided into two branches: one flowing west-southwest and the other southwest. The west-southwest branch developed into a channel with several rootless cone complexes located at its distal end ("VIII" in Figs. 4 and 5), whereas the southwest branch formed a lava pond within a topographic low ("N" in Fig. 5) and then generated several rootless cone complexes along its periphery. Up-flow from the lava pond, there is a prominent rootless cone with V-shaped trough along its axis ("O" in Fig. 5). To southeast of this rootless cone there is a linear alignment of rootless craters that extends for a distance of 50–55 m, at which point the craters exhibit a more widespread distribution. The region containing the widely distributed craters, termed subdomain 5.1 ("S5.1" in Fig. 5), contains 38 explosion sites within 36 explosion craters ranging 2.3–15.1 m in diameter with a mean of 6.9 m (σ = ±2.8 m, σ_e = ±1.1 m). To the east of subdomain 5.1, there is a tephra mantled kipuka (Fig. 5) and, to the south, rootless tephra deposits form a network of linearly aligned structures with conical to elongate morphologies ("IX" in Figs. 4 and 5).

Along the margins of the Hrossatungur group there are isolated rootless cones and cone complexes (e.g., "P" in Fig. 5). The lava that formed these rootless cones has flowed towards the Galti-Hrossatungur ridge from the periphery of the group, but the relative timing of its emplacement is poorly constrained.

Domain 6 In the northern part of domain 4, a coalesced series of explosion craters was occupied by a later lava flow to form a channel. Lava entered the coalesced chain of craters from the east and was deflected to the south by a paleotopographic high ("Q" in Fig. 5). The channelized lava widened to form a broad sheet lobe that generated rootless cones and lava-rafted tephra deposits. The rootless cones in domain 6 concentrate in subdomain 6.1 ("S6.1" in Fig. 5), which contains 130 rootless explosion sites within 124 craters. Rootless cones in subdomain 6.1 are smaller than in other regions of the Hnúta and Hrossatungur groups, with craters ranging 1.0–12.2 m in diameter and a mean of 4.1 m (σ = ±2.3 m, σ_e = ±0.4 m). Domain 6 is inferred to have the youngest rootless cones in the Hrossatungur group because they rest on a lava flow that overlies domain 4 and this flow also mantles rootless cones along the southern margin of domain 5. Rootless cones in domain 6 are primarily composed of spatter that has been deposited directly onto the surface of a lava flow to produce hornito-like structures. The cones and their craters are typically circular in plan view; however, there are excellent examples of elongated rootless cones with tephra wakes that formed by the deposition of spatter onto both sides of several lava channels, with rafted tephra accumulations developing in the down-flow direction ("X" in Figs. 4 and 5). There are also examples of rootless craters that have coalesced to form an open channel.

Tephrostratigraphy

Laki proximal tephrostratigraphy

Tephra sections in the vicinity of Mt. Hnúta show the stratigraphy of proximal Laki fall deposits (Thordarson 1990; Thordarson and Self 1993) and they provide critical information on the timing of rootless eruptions within the Hnúta and Hrossatungur groups. Each of the five sections that we excavated in the vicinity of Mt. Hnúta exhibit a similar depositional sequence and, therefore, we summarize the stratigraphy within one representative section (Fig. 6). At the base of the section, there is a 51.5 cm-thick bed (unit S1a) of black, coarse ash to coarse scoria lapilli that is clast-supported, reversely graded, and includes traces of Pele's hair. The modal grain-size in the lowermost 7.0 cm is fine lapilli, but increases to medium lapilli throughout the rest of the unit. The uppermost 5.0–6.5 cm of unit S1a mixes with material from the overlying layer (unit RCt1). Above this gradational contact, RCt1 forms a discrete 0.2–0.7 cm-thick bed of grey-brown fine ash with foreign cream colored pumice grains. Within this section, and three of the four other sections, RCt1 has a sharp contact with unit above (S1b); however, in one section there are traces of RCt1 within the lowermost 7.5 cm of S1b. Unit S1b is 61.0 cm thick and contains black, medium ash to medium lapilli scoria, which is clast-supported and contains traces of Pele's hair. The modal grain-size in the lowermost 8.0 cm is fine lapilli, whereas the modal grain-size above increases to medium lapilli for the bulk of the unit before approaching coarse lapilli in the uppermost 19 cm. The uppermost 2.0–3.5 cm of unit S1b mixes with tephra from the layer above (RCt2). RCt2 forms a 0.5–1.0 cm-thick layer containing grey-brown fine ash with traces of cream colored pumice. A sharp contact separates RCt2 from the overlying layer (unit S2). Unit S2 ranges 39–46 cm in thickness, with an average of 42 cm. Unit S2 consists of black, fine ash to coarse lapilli that is reversely graded, clast-supported, and includes abundant achneliths, Pele's hair, and Pele's tears. Clasts within unit S2 range from scoria to more highly

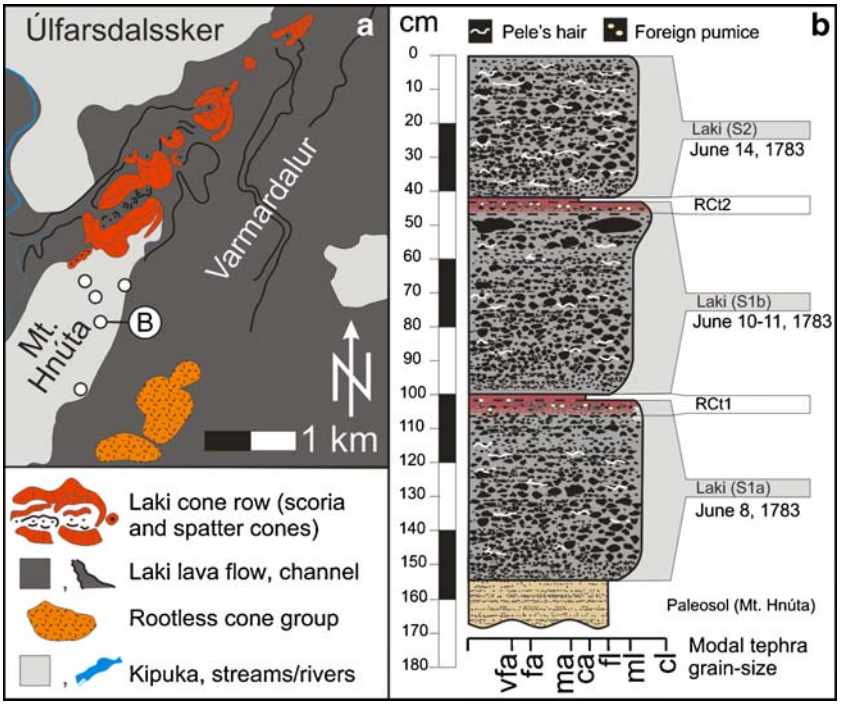

Fig. 6 Example of the Laki proximal tephra deposits at Mt. Hnúta, showing the stratigraphic relations between primary Laki fall units and fallout from the Hnúta-Hrossatungur rootless eruptions. Laki fall unit S1a was erupted from fissure segment 1 on June 8, S1b from fissure segment 2 on June 10–11, and S2 from fissure 3 on June 14, 1783. Rootless cone tephra (RCt) units include foreign pumice clasts excavated from the substrate. RCt1 is located between S1a and S1b with gradational contacts below and a sharp contact above, and RCt2 has a gradational lower contact with S1b and a sharp contact with S2. This indicates that there were at least two episodes of regional rootless tephra dispersal: RCt1, which initiated on June 8, but terminated before June 10; and RCt2, which began on June 11 and ended before June 14. The RCt1 deposits are attributed to sources within domain 1, whereas RCt2 is attributed to domain 2. The width of each layer corresponds to modal tephra grain size. Grain size abbreviations are as follows: coarse lapilli (cl); medium lapilli (ml); fine lapilli (fl), coarse ash (ca), medium ash (ma), fine ash (fa), and very fine ash (vfa)

vesicular golden pumice with ragged to blocky morphologies. The lowermost 7.0 cm of unit S2 has a modal grain-size of fine lapilli, which grades upwards to medium lapilli.

The lapilli beds represent primary magmatic tephra fall units from the Laki cone row. Although all of the scoria beds contain achneliths, the abundance of Pele's hair is greatest within unit S2. In the context of the established proximal stratigraphy for the Laki eruption (Thordarson and Self 1993; Thordarson et al. 2003), the lowest scoria bed (i.e., unit S1a), corresponds to tephra fall generated from fissure segment 1 on June 8, 1783, and unit S1b to the tephra fall from fissure segment 2 on June 10–11, 1783 (Fig. 1a and b). The high abundance of Pele's hair and Pele's tears in the scoria lapilli unit that caps the section is consistent with the characteristics of fall unit S2, which originated from fissure segment 3 on the June 14, 1783 (Thordarson and Self 1993). The two fine ash layers, RCt1 and RCt2, consist primarily of lusterless and poorly-vesicular ash fragments, brown mud, and foreign pumice grains. The well-rounded, cream-colored pumice clasts within RCt1 and RCt2, are atypical of all of the primary magmatic and phreatomagmatic Laki tephra units, and are most likely re-erupted material from the ~3900 B.C. Hekla S unit, which occurs as a prominent layer in the soil sections of the Laki region (Gudrun Larson, personal communication 2008).

The attributes of the RCt1 and RCt2 layers are consistent with the characteristics of fine fraction rootless tephra (Thordarson et al. 1998a). These rootless tephra layers most likely originate from sources in the Hnúta group or the Hrossatungur group, because of their proximity to Mt. Hnúta. The former is the most probable source because it contains larger craters, which imply more powerful eruptions and hence widespread tephra dispersal. Stratigraphic sections within the Hrossatungur group show rootless tephra in this region was deposited after S2 ("3" in Figs. 3 and 7) and thus after the emplacement of the Mt. Hnúta tephra section.

The position of RCt1 between fall units S1a and S1b, with a gradational contact below and a sharp contact above, implies rootless eruption activity initiated shortly after the beginning of the Laki eruption on June 8, but terminated prior to the initiation of S1b on June 10. RCt1 is most likely derived from rootless vents in the northern section of the Hnúta group (i.e., domain 1) because this region contains the oldest rootless cones. Given timing constraints on the emplacement of S1b and S2, RCt2 must have been

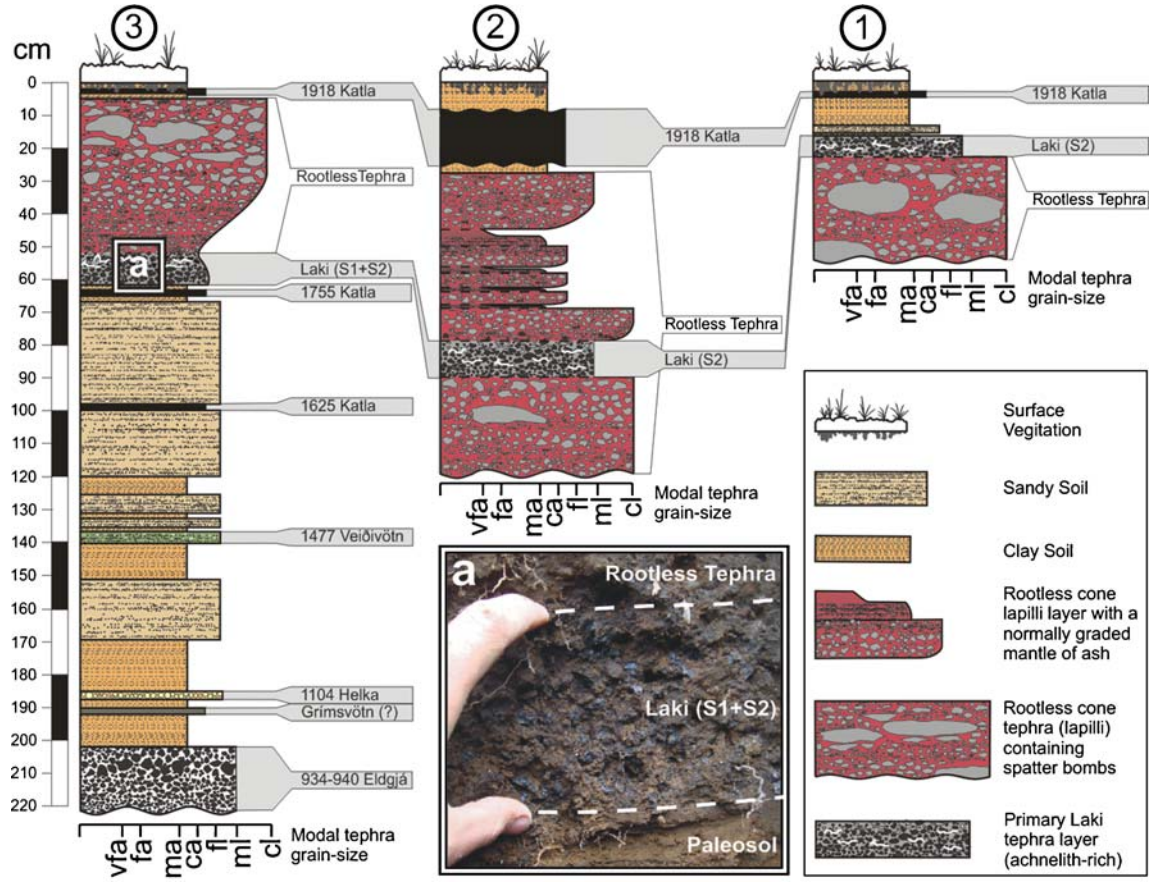

Fig. 7 Profiles through rootless tephra and underlying soil. **1:** A site in the central region of the lava labyrinth ("1" in Fig. 3). The S2 Laki fall unit rests on rootless tephra, implying rootless eruptions at this site terminated before the S2 phase (i.e., June 14. 1783). **2:** A site in the eastern lava labyrinth ("2" in Fig. 3). Unit S2 is interbedded with rootless tephra, indicating rootless eruptions at this site occurred through June 14. The bedding of the rootless tephra above the S2 unit implies cyclic activity and deposition during these rootless eruptions. **3:** Stratigraphic section near subdomain 5.1 ("3" in Fig. 3), showing rootless tephra resting on units S1 and S2, which indicates rootless eruptions in this vicinity occurred after June 14. The inset photograph (**a**) shows rootless tephra deposits overlying S1 and S2 units, which in turn overlie a pre-Laki paleosol. Deposition of Laki fall units directly onto surfaces that predate the Laki eruption confirms this site was a paleo-topographic high that was not inundated by lava. The caption of Fig. 6 explains the modal tephra grain size abbreviations

deposited during the final stages of S1b on June 11, but prior to the initiation of S2 on June 14. RCt2 most likely originates from rootless vents in the southern portion of the Hnúta group (i.e., domain 2). This conclusion is substantiated by the presence of rootless tephra below the magmatic fall unit S2 at a site in the central region of domain 2 ("1" in Figs. 3 and 7).

The tephrostratigraphy of the Hnúta and Hrossatungur groups

To identify kipuka, we excavated eighty-one pits and compared their tephrostratigraphy to the sequence of historical tephra layers exposed in our regional reference sections ("R" in Fig. 1a). Kipuka were positively identified if lava was not observed within a continuous soil sequence that included tephra layers pre-dating the Laki eruption. Identification of kipuka within the study area is important for reconstructing the paleo-environmental conditions that existed before the Laki eruption and for determining the influence of topography on rootless cone formation. The eighty-one excavation sites were also used to constrain the timing of rootless eruptions within the Hnúta and Hrossatungur groups by comparing the stratigraphic position of locally dispersed rootless tephra layers relative to historically documented fall deposits from the Laki cone row. We describe three stratigraphic sections in detail to demonstrate how we used tephrochronology to establish the timing of domain emplacement.

Tephra section 1 (Fig. 7), located within the central region of the lava labyrinth (domain 2; "1" on Fig. 3), contains rootless cone tephra overlain by a primary Laki fall unit, which is inferred to be unit S2 based on its thickness and componentry. domain 2 is stratigraphically younger than domain 1 and thus these two domains must have been emplaced before June 14, 1783—except in the eastern region

of the lava labyrinth where the S2 layer is present within a rootless tephra succession in tephra section 1 (Figs. 3 and 7). In tephra section 3 (Fig. 7), which was excavated into a kipuka adjacent to the eastern margin of subdomain 5.1 (Fig. 5), the S1 and S2 layers are located beneath the rootless cone deposits—indicating that rootless explosions in domain 5 commenced after the emplacement of the S2 unit (i.e., after June 14, 1783).

These observations are consistent with the proximal Laki tephrostratigraphy, which shows that the first rootless eruptions (RCt1)—interpreted to be from sources within domain 1—initiated late on June 8 and terminated before the opening of fissure segment 2 on June 10. The proximal Laki stratigraphy also shows a second phase of rootless eruptions (RCt2) beginning on June 11 and ceasing before June 14. This is in accord with the tephrostratigrapic record within tephra section 1 for the central region of domain 2. Rootless eruptions in the eastern portion of the lava labyrinth must have been of much lower intensity because rootless tephra generated after June 14 is not recorded within the Laki proximal stratigraphy. Similarly, tephra from the southern Hrossatungur group (domain 5) was erupted after June 14, but is not exposed within the Mt. Hnúta sections. This is understandable given the much lower intensity eruptions in this region relative to the Hnúta group.

Emplacement chronology of rootless cones within the Hnúta and Hrossatungur groups

Historical records (Thordarson 2003; Thordarson et al. 2003) and the distribution of kipuka (Fig. 5) suggest that prior to the Laki eruption there was a northeast–southwest trending ridge that ran between Galti and Hrossatungur (Fig. 1a). The Hnúta group is located at the southern end of Varmárdalur, along the northern slope of the Galti-Hrossatungur ridge, whereas the Hrossatungur group is situated near the axis of the ridge. The Síða branch of the Laki lava flow reached the vicinity of Mt. Leiðólfsfell on June 17, 1783—approximately 6 days after the Skaftá River gorge branch (Thordarson et al. 1998a). This delay can be attributed to the time it took lava from fissures 1–3 to flow south through Varmárdalur, mantle the boggy slopes of the Galti-Hrossatungur ridge, overtop the ridge, and continue its southward flow to Mt. Leiðólfsfell. Thus the emplacement chronology of rootless cone domains within the study area reflects the incremental inundation of topographic lows by lava flows during the Laki eruption. This general process was, however, complicated by local topographic inversions that were caused by lava inflation and rootless cone formation. In the following section, we present a reconstruction of the emplacement chronology for the six domains within the Hnúta and Hrossatungur groups (Fig. 3).

Domain 1 We propose that prior to the Laki eruption water ponded in a topographic basin between the southern end of Varmárdalur and the northern slope of the Galti-Hrossatungur ridge. We interpret this region to have been a marshy environment, or shallow lake, that was inundated by lava within hours of the opening of fissure 1 on June 8, 1783. To accommodate the influx of lava into Varmárdalur, the flow inflated and began to subside into the sedimentary substrate ("1" in Fig. 8). Subsidence resulted in flexure, failure, and extension of the basal lava crust, thereby allowing the molten interior of the flow to come into direct contact with the underlying groundwater. The resulting explosive lava–water interactions inverted the landscape by constructing the platform of the Hnúta group ("2" in Fig. 8). Given that RCt1 tephra mixes with the top of the Laki S1a unit, we conclude that rootless eruptions within domain 1 were triggered during the first day of the Laki eruption (i.e., June 8, 1783), and from the sharp contact that separates RCt1 from S1b, we infer that rootless eruptions within domain 1 terminated before June 10. The emplacement duration for domain 1 was therefore 1–2 days.

Broad flows initially fed widespread rootless eruptions within domain 1 (e.g., "B" in Fig. 3), but as a network of preferred lava pathways developed, the lava supply dwindled to many of the earlier formed rootless eruption sites because they were no longer supplied by the active lava transportation system. The pathways may initially have been lava tubes, but explosive activity locally disrupted the upper lava crust and allowed explosion craters to coalesce into open channels (e.g., "C" in Fig. 3). Spatter-rich tephra accumulated on both sides of the channels to form paired half-cone deposits with a V-shaped trough along the axis of the pathway. Tephra deposited onto the surface of the lava channel was either assimilated or rafted down-flow.

The transition from initially energetic and widespread explosive activity to low-energy (spatter-dominated) local tephra dispersal along lava pathways can be interpreted within the context of changing water-to-lava ratios (Wohletz 1983, 1986, 2002; Zimanowski et al. 1991; Zimanowski 1998). As the lava flow concentrated into preferred pathways, most of the platform-generating rootless eruption sites were starved of their fuel supply and thus could not sustain explosive activity. In contrast, along the preferred lava pathways there was an ample fuel, but as the local groundwater resources were depleted, the rootless eruptions became less intense and the explosive activity ultimately ceased.

Domain 2 The three arcuate deposits are attributed to at least three major rootless eruption sites that were active along the southern margin of the Hnúta group ("D", "E" and "F" in Fig. 3). Lava feeding these eruptions was funneled between Mt. Hnúta and the Hnúta group, but its progress was impeded by the Galti-Hrossatungur ridge.

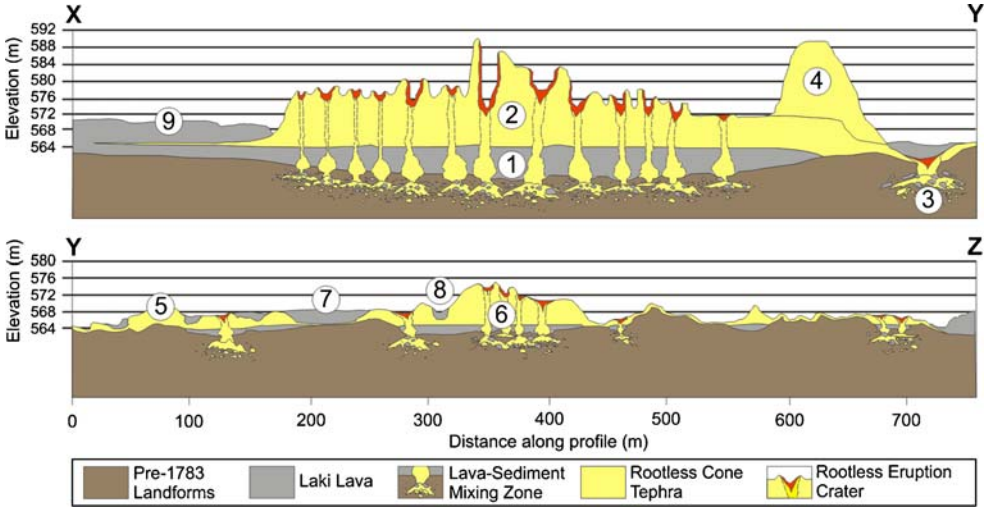

Fig. 8 Vertically exaggerated (×3.5) north–south cross-sections through the Hnúta (XY) and Hrossatungur (YZ) groups positioned to maximize the DGPS data density. **1:** Lava abuts the northern margin of the Galti-Hrossatungur ridge, inflates above a marshy paleo-topographic depression, and initiates explosive lava–water interactions. **2:** Rootless tephra accumulates to form the platform-like structure of domain 1. **3:** Rootless eruptions initiate in a lava branch that was deflected between domain 1 and the northern margin of the Galti-Hrossatungur ridge. These eruptions construct the arcuate ridge of domain 2 (**4**) and produce tephra accumulations within the lava labyrinth (**5**). **6:** Lava inundates the gullied northern slope of the Galti-Hrossatungur ridge and generates rootless eruptions to form domain 3. Domain 3 blocks the southward flow of lava, which then inflates in lava labyrinth (**7**) until it breaches the rootless cone barrier and resumes its flow toward the crest of the Galti-Hrossatungur ridge (**8**). Topographic inversions due to rootless cone formation temporarily block the through-flow of lava and thereby cause rubbly pahoehoe to develop along the northern margin of the Hnúta group (**9**). Features in the substrate are not shown to scale

Consequently, the lava inundated the topographic low formed between the southern margin of the Hnúta group platform and the north-facing slope of the ridge ("3" in Fig. 8). The rootless eruptions in this region dispersed tephra radially, but its preservation depended on the stability of the depositional surface in a fashion that is analogous to the formation of crescent-shaped ridges on stable landward surfaces during littoral eruptions. For instance, the material that was dispersed to the north accumulated along the southern margin of domain 1 to form a series of arcuate half-cone deposits ("4" in Fig. 8), whereas tephra ejected to the south was deposited onto both stable kipuka ("5" in Fig. 8) and unstable lava surfaces. Tephra deposited on the kipuka was preserved in situ, whereas material deposited on surface of moving lava flows was rafted down-flow to form labyrinthine accumulations of tephra with intervening lava pathways.

Funneling of lava between Mt. Hnúta and domain 1 promoted inflation and allowed the lava to inundate topographic lows at higher elevations. During this time isolated rootless eruptions were initiated as the lava accessed locations that had been protected previously by local topographic barriers. The superposition of the S2 Laki tephra horizon above rootless cone deposits in the center of lava labyrinth establishes that the cone-forming eruptions at this locality must have occurred before June 14, 1783. This is consistent with proximal Laki tephrostratigraphy, which shows a second major phase of rootless eruptions (RCt2) occurring late on June 11, but terminating before June 14. This implies that the main phase of activity within domain 2 lasted 1–3 days. In the eastern section of the lava labyrinth, the presence of the S2 layer in a rootless cone tephra succession shows that rootless eruptions occurred at this locality before and after June 14, 1783; however, given the limited dispersal of tephra from this region, we associate these eruptions with the waning stages of activity in domain 2.

Domain 3 The U-shaped cluster (i.e., domain 3) is one of the two oldest domains in the Hrossatungur group. The lava that generated these rootless cones flowed south from the lava labyrinth. The presence of kipuka to the east and west of domain 3 suggests that the flow entered a paleo-topographic depression that widened to the north. The geometry of this depression is consistent with the morphology that would be expected for a gully draining down along the northern slope of the Galti-Hrossatungur ridge. Rootless eruptions occurring along the margins of this gully caused a topographic inversion of the landscape ("6" in Fig. 8). On the up-flow side of domain 3, the lava was dammed within a reservoir that filled from the north. The flow continued to thicken and inundate small drainage channels along the northern slope of the Galti-Hrossatungur ridge (e.g., "K" in Fig. 5; "7" in Fig. 8) until the dammed lava achieved a critical thickness and overtopped the rootless cone craters in the northeastern section of domain 3. The lava flowed into

the central portion of domain 3 ("8" in Fig. 8) and was channeled towards the crest of the Galti-Hrossatungur ridge. When the flow reached the ridge crest, the lava entered two gullies that drained down along the southern slope of the ridge. Before discussing the consequences of this event, it is necessary to elaborate on other developments that were occurring to the east.

Domain 4 Domains 3 and 4 are separated by kipuka and therefore must be hosted by different lava lobes. Although they formed independently, the relative ages of these two subdomains cannot be determined on the basis of stratigraphic superposition because of coalescence of tephra from these two sources. Nevertheless, it is clear that these two rootless cone domains are of similar age and that they are the oldest within the Hrossatungur group because both domains are mantled by lava flows that host domains 5 and 6.

Domain 5 The rootless cones within the southern region of the Hrossatungur group are formed by lava that overlies domain 3 and, therefore, rootless cones in domain 5 must be younger. The lava flows in the vicinity of subdomain 5.1 occupy a paleo-topographic drainage network and generated rootless eruptions that locally inverted the landscape. Superposition of the rootless tephra above the S2 Laki layer shows that domain 5 was emplaced after June 14, 1783.

Domain 6 The emplacement of rootless cones in domain 4 temporarily halted the southward flow of lava though this region. The surrounding lava thickened until it inundated a coalesced series of eruption craters in the northeastern portion of subdomain 4.1. The lava flowed southwest until it encountered a paleo-topographic high and was redirected to the south. When the lava emerged in the south, it advanced over a water-bearing substrate and initiated a series of small explosions that constructed hornito-like spatter cones on the surface of the lava ("X" and "S6.1" in Figs. 4 and 5, respectively). The rootless cones in this region are exceptional due to their small size and almost exclusively spatter composition. The spatter-rich tephra suggests that groundwater, rather than lava, was the limiting reagent in these rootless eruptions. The small volume of the cones also implies that the substrate contained very little water relative to the other cone-forming regions in the study area.

Rubbly pahoehoe flows Throughout the stages discussed above, the platform of the Hnúta group presented a significant obstacle within the southward flowing lava. Topographic barriers limited the flux of lava through internal pathways and caused pressurization of the flow interior. When the applied stress from the pressurized molten core exceeded the yield strength of the overlying viscoelastic layer, the lava surface was disrupted into slabs. The lava surface developed into a rubbly pahoehoe flow as the fractured slabs of crust continued to fragment and accumulated at the flow front (Keszthelyi et al. 2004; Guilbaud et al. 2005). Compression of the southward moving flow against the Hnúta group caused a series of arcuate ridges to develop on the flow surface (Fig. 1c and "9" in Fig. 8). Restricted flow between the Hnúta group and Mt. Hnúta caused the lava to stagnate and solidify in this region, thereby diverting subsequent flows to the southeast. The redirection of the flow reduced the supply of lava through the Hrossatungur group and generally resulted in lava drainage and subsidence, but the presence of post-subsidence tumuli implies that some lava pathways remained active for a longer period of time. This lava supply may have been fed to the south beneath a carapace of rubbly pahoehoe that extends between Mt. Hnúta and the western margin of Hnúta and Hrossatungur groups.

Rootless cone archetypes

In general, rootless cones divide into aligned and non-aligned archetypes. Cone alignment depends upon the geometry of the host lava lobe and the lava transportation system within it. In this context, we define two end-member geometries: (1) narrow pathways, including both lava tubes and channels, which tend to form aligned rootless cones; and (2) sheet lobes with a broad unconfined lava transport system that generate unaligned cones. As a lava lobe matures, an initially broad lava transportation system will concentrate into preferred pathways (Mattox et al. 1993; Kauahikaua et al. 1998; Self et al. 1998); however, the reverse is not possible. If a sheet lobe develops a network of pathways, linearly aligned cones may be superimposed onto dispersed rootless cone clusters as we have observed within the Hnúta group (Fig. 3).

Aligned rootless cones

Cone alignments may result from tube- and channel-fed rootless eruptions. Tephra deposited onto the stationary lava surface above a lava tube tends to construct radially symmetrical cones (Fig. 9a), whereas tephra deposited over lava channels will generally form a rootless cone with a V-shaped trough along the pathway axis (Fig. 9b). Discrete rootless eruption sites produce isolated rootless cones with radial symmetry; however, within the Hrossatungur group, it is more common for lava tubes and channels to host a series of eruption sites with ejecta that merges to form elongate structures (Fig. 5). Channel-hosted rootless cones develop an axial trough bound by cone ramparts due to

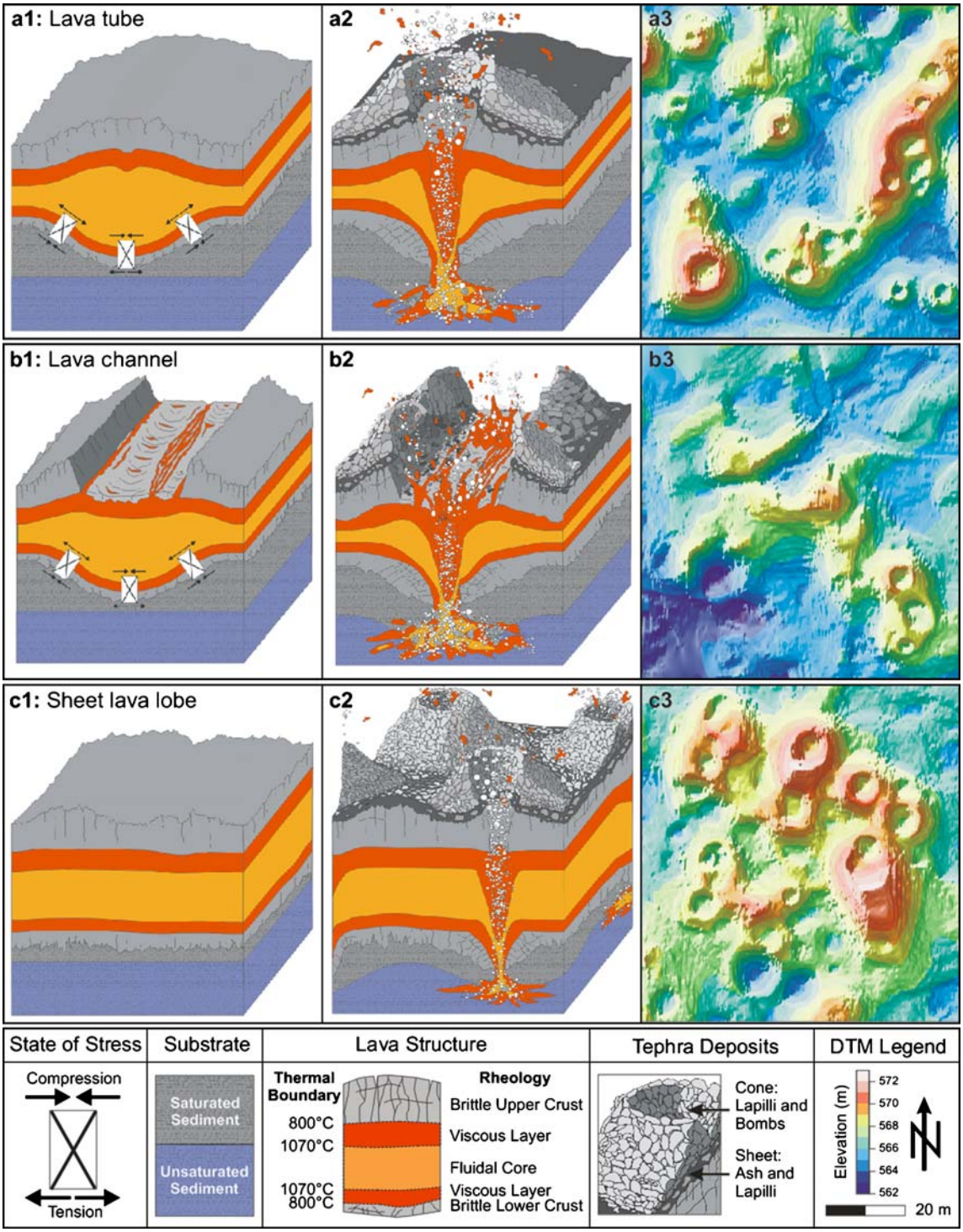

Fig. 9 Tube-fed (**a**), channel-fed (**b**), and sheet lobe-fed (**c**) archetypes. Narrow lava pathways include lava tubes and channels, which may subside into a compressible substrate and generate a maximum tensile stress along the flow axis (**a1** and **b1**). As the basal crust opens by extension, lava within the viscoelastic layer and fluidal core can deform through fractures to come into direct contact with the wet substrate. Tephra generated by tube-fed explosions accumulates on the stationary upper surface of the flow and may either exhibit radial symmetry or elongation along the tube axis (**a3**). During channel-fed explosions (**b2**) pyroclasts can be deposited onto the surface of the active channel and transported down-flow to produce rootless tephra deposits with a paired half-cone morphology that only preserves material along the stationary channel levees (**b3**). Broad sheet lobes (**c1**) do not have a geometrically controlled state of stress that favors rootless cone alignments. Flow through broad zones of lava emplacement may bypass local blockages and thereby sustain multiple simultaneous rootless eruptions (**c2**) to produce rootless tephra complexes (**c3**). a3, b3, and c3 are plan view Digital Terrain Models (DTMs) of rootless cones in the vicinity of subdomain 5 (Hamilton et al. 2010)

down-flow rafting of tephra that has been deposited onto a moving lava surface (e.g., "X" in Fig. 4). The resulting paired half-cone morphology is also common among channel-fed littoral cones (Jurado-Chichay et al. 1996; Mattox and Mangan 1997).

Narrow pathway geometries favor rootless cone alignments because the state of stress at the base of the lava flow generates failure along an axial zone. An advancing pahoehoe flow rapidly develops a layered rheological structure that includes a brittle crust surrounding a viscoeleastic layer, which in turn surrounds a fluid core (Hon et al. 1994). The brittle basal crust may initially support the mass of the flow, but the development of cooling fractures weakens the basal layer (Thordarson and Self 1998b). At this point, the strength of the flow is derived from the viscoelastic layer, much like an egg with a cracked shell is supported by the underlying membrane. If the lava rests on a compressible substrate it may subside. Narrow pathways are best approximated by a cylindrical geometry with a maximum tensile stress exerted along its longitudinal axis (Fig. 9a1). As it subsides into the substrate, the brittle crust opens by cracking and extension and enables the viscoelastic layer and molten core to extrude through the fractures. This failure zone beneath a narrow pathway is thus analogous to the axial cleft on an elongate tumulus (Walker 1991; Rossi and Gudmundsson 1996).

If molten lava extrudes through the fractures in the basal crust and comes into direct contact with a water-bearing substrate, explosive lava–water interactions may initiate and excavate a conduit to the surface of the lava flow. The pyroclasts ejected in repeated explosions then accumulate as a rootless cone on the stationary surface of the lava (Fig. 9a2). Rootless eruptions typically destroy the lava pathway in their vicinity, which often results in enhanced inflation in the up-flow segment of the lava tube. Enhanced up-flow inflation increases the applied stresses on the basal viscoelastic layer and may trigger the initiation of new failure zones. This cycle of activity may result in up-flow migration of active eruption sites to produce an alignment of rootless cones (Fagents and Thordarson 2007). Figure 9a3 provides examples of isolated and elongate rootless cones that have been constructed upon the stationary lava surface above a network of lava tubes.

Tube- and channel-fed archetypes can combine to produce transitional rootless cone morphologies. For instance, a series of rootless eruption sites may disrupt the rigid surface of a lava tube to produce an open channel. Alternatively, an open lava channel may develop a stationary crust and thereby form a tube. These transitions may either occur in time or along the length of given lava pathway. For example, a change from a linear chain of rootless craters with interfingered radially symmetric tephra deposits to an elongated structure with a prominent axial trough (e.g., "R" in Fig. 5) may reflect a transition from a tube to an open channel along the same lava pathway. The "chute and pool" geometry of most lava tubes (e.g., Guest et al. 1984; Calvari and Pinkerton 1999) and, to a lesser extent, lava channels (e.g., Woodcock and Harris 2006; Harris et al. 2009) may complicate simple rootless cone alignments by generating a state of stress that favors failure at the base of the flow along off-axis sites. Isolated rootless cones may also form in association with tumuli above pools in an internal pathway system (e.g., "H" in Fig. 5), which supports the conclusion that rootless cones form in sites of enhanced inflation.

Non-aligned rootless cones

In contrast to narrow pathways, which tend to produce isolated rootless cones and coalesced cones with an elongate morphology, broad sheet lobes can host non-aligned rootless groups. These rootless cones may appear isolated and distinct from one another, as is observed within subdomain 6.1 of the Hrossatungur group ("S6.1" in Fig. 5), but in most instances they have coalesced to form rootless cone complexes (e.g., "S3.1", "S4.1", and "S5.1" in Fig. 5) or platforms (e.g., the Hnúta group, Fig. 3). Rootless cones hosted within broad sheet flows generally lack alignments and may include numerous, simultaneously active eruption sites because the lava transportation system is not constricted and can thus bypass local blockages caused by rootless explosions. The conditions required to initiate failure zones within broad flows are not well characterized, but are most likely governed by topographic irregularities, heterogeneous substrate compressibility, and flow emplacement history.

Conclusions

Rootless cone groups are composite structures formed by the incremental emplacement of discrete domains. Consequently, adjacent domains may be formed at different times and under different environmental conditions. In the Hnúta and Hrossatungur groups, pre-eruption topography provided a regional control on the spatial distribution of rootless eruption sites. Topographic influences were important because they affected the initial distribution of groundwater and the zones of lava inundation during the Laki eruption. In regions where rootless cones formed, we propose that the Laki lava advanced over compressible substrates. Molten fuel–coolant interactions (MFCIs) were then generated by subsidence-induced flexure and failure of the basal lava crust, which allowed molten lava (fuel) to extrude through extensional fractures and come into direct contact with underlying groundwater (coolant). This conceptual model provides an alternative to phreatic triggering mechanisms that require conductive heat transfer to

continue through a stable interface at the base of a lava flow until the pressure within an accumulated layer of vapor exceeds the mechanical strength of the overlying lava flow and its overburden pressure.

By using local contact relationships and tephrochronology we have established that the Hnúta group was emplaced during two phases. The first rootless eruption phase began on June 8, 1783 and constructed domain 1 within 1–2 days. The second phase initiated on June 10 and formed domain 2 within 1–3 days. The Hrossatungur group, located further to the south, includes four constituent domains that all began to form after the emplacement of domain 2. The general southward migration of active rootless eruption sites within the study area reflects the progressive inundation of water-bearing topographic lows by the Laki lava as it thickened and advanced over the Galti-Hrossatungur ridge. The Hnúta group, which contains the largest rootless cones in the study area, formed near the northern foot of the ridge—above a basin that we interpret to have been a marsh or shallow lake. The Hrossatungur group formed at higher elevations when the Laki lava flowed into a network of gullies that drained the slopes of the Galti-Hrossatungur ridge. Within some of the gullies there was sufficient near-surface water to generate rootless eruptions. In contrast to the Hnúta group, which exhibits an overall platform morphology, the Hrossatungur group consists of smaller rootless cones that are separated by kipuka. Divergence in rootless cone morphologies within these two groups reflects differences in the abundance of water in the underlying substrate and the modes of lava emplacement—both of which are correlated with paleo-topography.

The Hnúta group was dominantly constructed by broad sheet lobe-fed eruptions, but as the flow matured, it developed a series of tubes and channels that starved the lava supply to regions that were removed from the preferred pathways. Along the active pathways there was a continuous supply of lava and rootless eruptions were limited by the depletion of underlying groundwater. Within the Hrossatungur group, rootless cones include aligned and non-aligned archetypes. Aligned archetypes are interpreted to be the result of rootless eruptions that occurred along the axis of narrow lava tubes and channels. The spatial distribution of tube- and channel-fed rootless eruptions will largely depend on the geometry of the underlying lava pathway, whereas broad sheet lobes have a more widely distributed lava supply and may generate non-aligned rootless eruption sites.

Using the group, domain, and subdomain boundaries established within this study, Hamilton et al. (2010) explore the physical processes that affect the spatial distribution of rootless eruption sites. Their results suggest that on a regional scale rootless cones cluster into groups and domains, but within subdomains rootless eruption sites tend to self-organize into distributions that maximize the utilization of limited groundwater resources. In our companion paper (Hamilton et al. 2010), we also compare volcanic rootless cones in the Hnúta and Hrossatungur groups to analogous landforms in the Tartarus Colles Region of Mars. Both sets of landforms exhibit similar morphological and geospatial characteristics, which suggests a similar underlying formation mechanism through explosive lava–water interactions.

Acknowledgements We thank Karen Pascal for her assistance in the field; Benjamin Brooks and the Pacific GPS facility for providing DGPS survey equipment and post-processing resources; Bruce Houghton and Scott Rowland for their help during the preparation of this manuscript; Bernd Zimanowski and an anonymous reviewer for their encouraging comments and suggestions; and financial support from the National Aeronautics and Space Administration (NASA) Mars Fundamental Research Program (MFRP) grant NNG05GM08G, NASA Mars Data Analysis Program (MDAP) grant NNG05GQ39G, Geological Society of America (GSA), and Icelandic Centre for Research (RANNÍS). SOEST publication number 7807. HIGP publication number 1801.

References

Allen CC (1979) Volcano-ice interactions on Mars. J Geophys Res 84:8048–8059

Brigham WT (1868) The eruption of Hawaiian volcanoes. Boston Soc Natl Mem 1:564–587

Calvari S, Pinkerton H (1999) Lava tube morphology on Etna and evidence for lava flow emplacement mechanisms. J Volcanol Geotherm Res 90:263–280

Colgate SA, Sigurgeirsson T (1973) Dynamic mixing of water and lava. Nature 244:552–555

Fagents SA, Lanagan P, Greeley R (2002) Rootless cones on Mars: a consequence of lava-ground ice interaction. In: Smellie JL, Chapman MG (eds) Volcano-ice interaction on Earth and Mars. Geol Soc Spec Publ 202:295–317

Fagents SA, Thordarson T (2007) Rootless volcanic cones in Iceland and on Mars. In: Chapman MG (ed) The geology of Mars: evidence from Earth-based analogs. Cambridge University Press, New York, pp 151–177

Fisher RV (1968) Pu'u Hou littoral cones, Hawaii. Geol Rundsch 57:837–864

Fisher RV, Schmincke H-U (1984) Pyroclastic rocks. Springer-Verlag, New York

Frey H, Lowry BL, Chase SA (1979) Pseudocraters on Mars. J Geophys Res 84:8075–8086

Frey H, Jarosewich M (1982) Subkilometer Martian volcanoes: properties and possible terrestrial analogs. J Geophys Res 87:9867–9879

Greeley R, Fagents SA (2001) Icelandic pseudocraters as analogs to some volcanic cones on Mars. J Geophys Res 106:20527–20546

Guest JE, Wood C, Greeley R (1984) Lava tubes, terraces and megatumuli on the 1614–24 pahoehoe lava flow field, Mount Etna, Sicily. Bull Volcanol 47:635–648

Guilbaud MN, Self S, Thordarson T, Blake S (2005) Morphology, surface structures, and emplacement of lavas produced by Laki, A.D. 1783–1784. Geol Soc Am Spec Pap 396:81–102

Hamilton CW, Fagents SA, Thordarson T (2010) Explosive lava–water interactions II: self-organization processes among volcanic

rootless eruption sites in the 1783–1784 Laki lava flow, Iceland. Bull Volcanol. doi:10.1007/s00445-009-0331-5
Harris JL, Favalli M, Mazzarini F, Hamilton CW (2009) Construction dynamics of a lava channel. Bull Volcanol 71:459–474. doi:10.1007/s00445-008-0238-6
Hon K, Kauahikaua J, Denlinger R, MacKay R (1994) Emplacement and inflation of pahehoe sheet flows: observations and measurements of active lava flows on Kilauea Volcano, Hawaii. Geol Soc Am Bull 106:351–370
Jurado-Chichay Z, Rowland SK, Walker GPL (1996) The formation of circular littoral cones from tube-fed pahoehoe: Mauna Loa, Hawaii. Bull Volcanol 57:471–482
Kauahikaua J, Cashman KV, Mattox TN, Heliker CC, Hon KA, Mangan MT, Thornber CR (1998) Observations on basaltic lava streams in tubes from Kilauea Volcano, island of Hawai'i. J Geophys Res 103:27303–27323
Keszthelyi L, Thordarson T, McEwen A, Haack H, Guilbaud M-N, Self S, Rossi MJ (2004) Icelandic analogs to Martian flood lavas. Geochem Geophys Geosyst 5:Q11014. doi:10.1029/2004GC000758
Lanagan PD, McEwen AS, Keszthelyi LP, Thordarson T (2001) Rootless cones on Mars indicating the presence of shallow equatorial ground ice in recent times. Geophys Res Lett 28:2365–2367
Mattox TN, Mangan MT (1997) Littoral hydrovolcanic explosions: a case study of lava-seawater interaction at Kilauea volcano. J Volcanol Geotherm Res 75:1–17
Mattox TN, Heliker C, Kauahikaua J, Hon K (1993) Development of the 1990 Kalapana flow field, Kilauea Volcano, Hawai'i. Bull Volcanol 55:407–413
Mellon MT, Jakosky BM (1995) The distribution and behavior of martian ground ice during past and present epochs. J Geophys Res 100:11781–11799
Morrissey M, Zimanowski B, Wohletz K, Buettner R (2000) Phreatomagmatic fragmentation. In: Sigurdsson H, Houghton B, McNutt S, Rymer H, Stix J (eds) Encyclopedia of volcanoes. Academic, New York, pp 431–445
Pálsson S (1794) Ferðabók Sveins Pálssonar, Dagbækur og Ritgerðir 1791–1797, 2nd edition. Örn og Örlygur, Reykjavík
Robert E (1840) P. Gaimard voyage en Islande et au Grönlande. Mineralogie et Geologie, Paris
Rossi MJ, Gudmundsson A (1996) The morphology and formation of flow-lobe tumuli on Icelandic shield volcanoes. J Volcanol Geotherm Res 72:291–308
Self S, Keszthelyi L, Thordarson T (1998) The importance of pahoehoe. Ann Rev Earth Planet Sci 26:81–110
Squyres SW, Clifford SM, Kuzmin RO, Zimbelman JR, Costard FM (1992) Ice in the Martian regolith. In: Kieffer HH, Jakosky BM, Snyder CW, Mathews MS (eds) Mars. University of Arizona Press, Tucson, pp 523–554
Steingrímsson J (1788) Fulkomid Skrif um Sídueld. Safn til Sögu Íslands IV:8–69
Steingrímsson J, Ólafsson S (1783) Einföld og sönn frásaga um jardeldshlaupid í Skaftafellssyslu árid 1783. Safn til Sögu Íslands IV:58–69
Thorarinsson S (1951) Laxargljufur and Laxarhraun: a tephrachronological study. Geograf Annal H1(2):1–89
Thorarinsson S (1953) The crater groups in Iceland. Bull Volcanol 14:3–44
Thordarson T (1990) The eruption sequence and eruption behavior of the Skaftár Fires, 1783–85, Iceland: characteristics and distribution of eruption products. MS thesis, University of Texas at Arlington, Arlington
Thordarson T, Self S (1993) The Laki (Skaftar Fires) and Grimsvotn eruptions in 1783–85. Bull Volcanol 55:233–263
Thordarson T, Self S, Oskarsson N, Hulsebosch T (1996) Sulfur, chlorine, and fluorine degassing and atmospheric loading by the 1783–1784 AD Laki (Skaftár Fires) eruption in Iceland. Bull Volcanol 58:205–225
Thordarson T, Miller DJ, Larsen G (1998a) New data on the Leidolfsfell cone group in South Iceland. Jökull 46:3–15
Thordarson T, Self S (1998b) The Roza Member, Columbia River Basalt Group: a gigantic pahoehoe lava flow field formed by endogenous processes? J Geophys Res 103:27411–27445
Thordarson T (2003) The 1783–1785 A.D. Laki-Grímsvötn eruptions I: a critical look at the contemporary chronicles. Jökull 53:1–10
Thordarson T, Self S (2003) Atmospheric and environmental effects of the 1783–1784 Laki eruption: a review and reassessment. J Geophys Res 108(D1):4011. doi:10.1029/2001JD002042
Thordarson T, Larsen G, Stienþórsson S, Self S (2003) The 1783–1785 A.D. Laki-Grímsvötn eruptions II: appraisal based on contemporary accounts. Jökull 53:11–47
Thoroddsen T (1879) Volcanic eruptions in Iceland in the year 1783. Geografisk Tidskrift 3:67–80
Thoroddsen T (1894) Ferð um Vestur–Skaptafellssýslu sumarið 1893. Andvari 19:44–161
Walker GPL (1991) Structure, and origin by injection of lava under surface crust, of tumuli, `lava rises´, `lava-rise pits´, and `lava-inflation clefts´ in Hawaii. Bull Volcanol 53:546–558
Wohletz KH, Sheridan MF (1983) Hydrovolcanic explosions II. Evolution of basaltic tuff rings and tuff cones. Am J Sci 283:385–413
Wohletz KH (1983) Mechanisms of hydrovolcanic pyroclast formation: size, scanning electron microscopy, and experimental studies. J Volcanol Geotherm Res 17:31–63
Wohletz KH (1986) Explosive magma-water interactions: thermodynamics, explosion mechanisms, and field studies. Bull Volcanol 48:245–264
Wohletz KH (2002) Water/magma interaction: some theory and experiments on peperite formation. J Volcanol Geotherm Res 114:19–35
Woodcock D, Harris AJL (2006) The dynamics of a channel-fed lava flow on Pico Partido volcano, Lanzarote: evidence for a hydraulic jump? Bull Volcanol 69:207–125
Zimanowski B, Fröhlich G, Lorenz V (1991) Quantitative experiments on phreatomagmatic explosions. J Volcanol Geotherm Res 48:341–358
Zimanowski B (1998) Phreatomagmatic explosions. In: Freundt A, Rosi M (eds) From magma to tephra. Elsevier, Amsterdam, pp 25–554